

P- and T-violating πNN form factor

S. Kondratyuk and P. G. Blunden

*Department of Physics and Astronomy,
University of Manitoba, Winnipeg, MB, Canada R3T 2N2*

(Dated: July 23, 2018)

Abstract

The form factor of the parity and time-reversal violating (PTV) pion-nucleon interaction is calculated from one-loop vertex diagrams. The degrees of freedom included in the effective lagrangian are nucleons, pions, η , ρ and ω mesons. We show that by studying the form factor one can constrain the PTV meson-nucleon coupling constants. We evaluate the mean square radius associated with the PTV πNN vertex. Using the mean square radius, we estimate the effect of the PTV πNN vertex on the neutron electric dipole moment, and find a very small correction. We also extract the renormalisation group β function and use it to discuss evolution of the PTV πNN coupling constant beyond the hadronic mass scale.

PACS numbers: 11.30.Er, 13.75.Gx, 24.80.+y

I. INTRODUCTION

The parity (P) and time-reversal (T) nonconserving pion-nucleon coupling is a theoretical ingredient in many calculations of electric dipole moments (EDMs) of various systems, such as the neutron, deuteron, various atoms and molecules [1]. The continuing interest in the problem of EDMs, and its relevance to possible extensions of the Standard Model [2], is a major motivation for a deeper understanding of the P- and T-violating (PTV) πNN interaction. Usually in calculations one uses a point-like PTV πNN interaction, neglecting a form factor associated with effects of nonlocality.

In this paper we calculate such a form factor from meson loop corrections to a bare PTV πNN vertex. The loop integrals are evaluated in a relativistic field theoretical approach based on an effective lagrangian comprising the nucleon, pion, ρ , ω and η mesons. The lagrangian consist of a strong interaction piece involving in principle well-known coupling constants, and a PTV piece involving unknown coupling constants. Our aim is to study various features of the calculated PTV πNN form factor – for example, its dependence on the square of the momentum transferred by the pion to the nucleon, the associated mean square radius, etc. Using renormalisation group methods in a one-loop approximation, we also consider possible scenarios of the high-energy evolution of the PTV πNN constant. The latter problem in particular is motivated by the puzzle of the extremely small value of the charge and parity (CP) violating θ term in the QCD lagrangian [2]. Throughout the paper, we do not assign specific numerical values to the unknown PTV meson-nucleon coupling constants. We do, however, make general assumptions as to the relations among them (e. g. choosing the constants to be of comparable magnitude or assuming some of them to be suppressed) and analyse consequences of these assumptions for the PTV πNN form factor, the mean square radius and the high-energy scale evolution of the PTV coupling constant.

Our results could be used to study effects of the PTV πNN form factor in calculations of electric dipole moments of the nucleon. We will make a tentative estimate indicating that the PTV πNN form factor introduces a very small correction to a leading chiral contribution to the neutron EDM. To our knowledge, a measurement of a PTV πNN form factor has not been attempted so far. We will show that such a measurement could, in particular, put some constraints among the PTV meson-nucleon coupling constants. Since at present such experimental applications are rather speculative, in this paper we will focus on the PTV form factor itself, leaving specific calculations of related measurable PTV amplitudes for future research.

II. EFFECTIVE LAGRANGIAN

The interaction among hadrons in our model is described by the sum of the strong lagrangian \mathcal{L}_S and the P-,T-violating lagrangian \mathcal{L}_{PT} [3]:

$$\mathcal{L} = \mathcal{L}_S + \mathcal{L}_{PT}, \quad (1)$$

where

$$\begin{aligned} \mathcal{L}_S = & \frac{g_\pi}{2M} \bar{N} \gamma_5 \gamma_\mu \boldsymbol{\tau} \cdot (\partial^\mu \boldsymbol{\pi}) N + \frac{g_\eta}{2M} \bar{N} \gamma_5 \gamma_\mu (\partial^\mu \eta) N + i g_{\rho\pi} \boldsymbol{\rho}_\mu \cdot [\boldsymbol{\pi} \times \partial^\mu \boldsymbol{\pi}] \\ & + g_\rho \bar{N} \left\{ (\gamma^\mu - \frac{\kappa_\rho}{2M} \sigma^{\mu\nu} \partial_\nu) \boldsymbol{\tau} \cdot \boldsymbol{\rho}_\mu \right\} N + g_\omega \bar{N} \left\{ (\gamma^\mu - \frac{\kappa_\omega}{2M} \sigma^{\mu\nu} \partial_\nu) \omega_\mu \right\} N, \end{aligned} \quad (2)$$

$$\begin{aligned}
\mathcal{L}_{\mathcal{PT}} &= \overline{N} \left\{ \overline{g}_\pi^{(0)} \boldsymbol{\tau} \cdot \boldsymbol{\pi} + \overline{g}_\pi^{(1)} \pi^0 + \overline{g}_\pi^{(2)} \tau_3 \pi^0 \right\} N + \overline{N} \left\{ \overline{g}_\eta^{(0)} \eta + \overline{g}_\eta^{(1)} \tau_3 \eta \right\} N \\
&+ \frac{i}{2M} \overline{N} \left\{ \sigma^{\mu\nu} \gamma_5 \partial_\nu \left[\overline{g}_\rho^{(0)} \boldsymbol{\tau} \cdot \boldsymbol{\rho}_\mu + \overline{g}_\rho^{(1)} \rho_\mu^0 + \overline{g}_\rho^{(2)} \tau_3 \rho_\mu^0 \right] \right\} N \\
&+ \frac{i}{2M} \overline{N} \left\{ \sigma^{\mu\nu} \gamma_5 \partial_\nu \left[\overline{g}_\omega^{(0)} \omega_\mu + \overline{g}_\omega^{(1)} \tau_3 \omega_\mu \right] \right\} N
\end{aligned} \tag{3}$$

(our constants $\overline{g}_{\pi,\rho}^{(0)}$ and $\overline{g}_{\pi,\rho}^{(2)}$ are equal to $\overline{g}_{\pi,\rho}^{(0)} - \overline{g}_{\pi,\rho}^{(2)}$ and $3\overline{g}_{\pi,\rho}^{(2)}$, respectively, as defined in Ref. [3]). The nucleon field is denoted as N ; the pion, ρ , ω and η meson fields as π^i , ρ_μ^i , ω_μ and η , respectively, with the lower indices denoting Lorentz vector components and the upper indices isovector components; the bold font indicates isovectors and τ_i are the Pauli isospin matrices.¹ The hadron masses are: $M = 0.938$ GeV for the nucleon, $m = 0.138$ GeV for the pion, $m_\rho = 0.77$ GeV, $m_\omega = 0.78$ GeV, $m_\eta = 0.55$ GeV for the other mesons. The coupling constants in the strong lagrangian \mathcal{L} are chosen as in Ref. [3]: $g_\pi = 13.07$, $g_\eta = 2.24$, $g_\rho = 2.75$, $\kappa_\rho = 3.7$, $g_\omega = 8.25$, $\kappa_\omega = -0.12$ and $g_{\rho\pi} = 6.07$ (from the width of the ρ resonance [5]).

Retaining all isospin structures in the PTV πNN (and other meson-nucleon) vertices would involve many unknown coupling constants, which would make results of loop calculations based on the lagrangian Eq. (3) difficult to interpret. Therefore, to keep our analysis tractable, in the following we will consider only the $\sim \overline{g}_\pi^{(0)}$ isospin structure in the PTV πNN vertex, which involves a charged pion and therefore appears in the calculations of the neutron EDM [3, 6]. We will use the simplified notation for the renormalised (physical) coupling constants: $c_\pi = \overline{g}_\pi^{(0)}$, $c_\rho = \overline{g}_\rho^{(0)}$, $c_\omega = \overline{g}_\omega^{(0)}$, $c_\eta = \overline{g}_\eta^{(0)}$. Note that the PTV πNN coupling constant in the lagrangian Eq. (3) is a bare constant c_π^B which will serve to cancel infinities of the loop integrals in the course of renormalisation described in the next section.

We use the pseudovector (pv) strong πNN vertex in Eq. (2). The pseudoscalar (ps) structure $ig_\pi \overline{N} \gamma_5 \boldsymbol{\tau} \cdot \boldsymbol{\pi} N$ is also used in the literature on effective lagrangian calculations of effects of parity and time reversal violation [3, 6]. The pv structure of the πNN vertex was used in the recent chiral calculation [7] of the nucleon electric dipole form factor. While the ps and pv couplings are equivalent on shell, the pseudovector is more consistent with chiral constraints, which motivates our choice. In the course of the discussion below we will specify important differences and similarities between the results obtained using the pv and the ps strong πNN vertices.

III. ONE-LOOP VERTEX DIAGRAMS GENERATING THE FORM FACTOR

We calculate the vertex loop diagrams depicted in Fig. 1, for the space-like pion momenta, $q^2 \equiv -Q^2 \leq 0$, and with both nucleons on-shell.

Before renormalisation, the PTV vertex can be written as $c_\pi^B + \Gamma^B(q^2)$, which is the sum of the tree-level contribution c_π^B from the lagrangian Eq. (3) and the bare (unrenormalised) one-loop corrections $\Gamma^B(q^2)$. To render the calculated loop integrals $\Gamma^B(q^2)$ ultraviolet convergent, we apply the modified minimal subtraction procedure in conjunction with dimensional regularisation [8, 9]. This procedure amounts to setting the constant Δ (defined in Appendix A), which is divergent in the limit $D \rightarrow 4$, to zero in the unrenormalised loops $\Gamma^B(q^2)$. In this way we obtain ultraviolet and infrared convergent loop integrals which do

¹ All other conventions and definitions used throughout this paper follow Ref. [4].

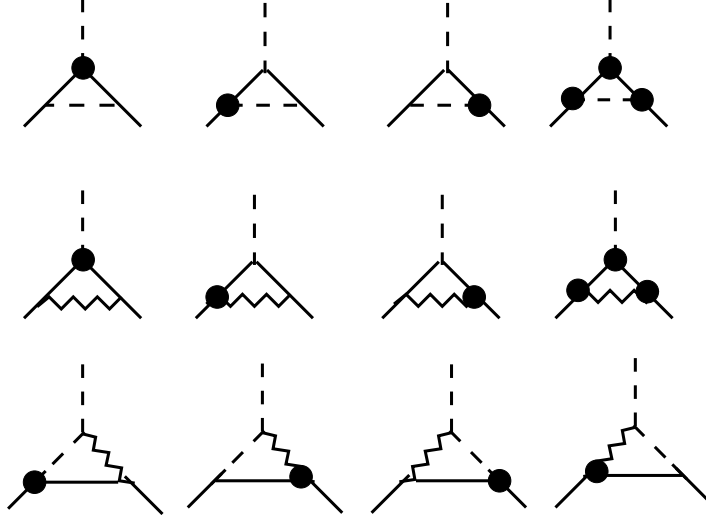


FIG. 1: The loop diagrams included in the calculation of the P- and T-violating πNN form factor. The solid and dashed lines denote nucleons and pions, respectively. In addition, in the upper row, the internal dashed lines are π or η mesons, and in the middle row, the zigzag lines are ρ or ω mesons. The blobs represent the PTV interactions from Eq. (3), and the other vertices denote the strong interactions from Eq. (2).

not depend on the regularisation parameters (see Appendix A): the dimension D (which after renormalisation can be set to the physical value $D = 4$) and the interim cutoff Λ (which may be thought of as a scale much larger than the included hadronic masses). The renormalisation can be interpreted as an absorption of the infinities of the unrenormalised loops $\Gamma^B(q^2)$ into the bare coupling constant c_π^B , such that the full vertex is rewritten as the sum of a renormalised coupling constant c_π and a renormalised loop contribution $\Gamma(q^2)$, both of them free of infinities. The PTV πNN form factor $F_{PT}(Q^2)$ is then defined by

$$c_\pi + \Gamma(q^2) = c_\pi F_{PT}(Q^2). \quad (4)$$

The sum of the renormalised loop diagrams with an intermediate pion reads

$$\Gamma_\pi(q^2) = \frac{c_\pi g_\pi^2}{16\pi^2} \left\{ V_\pi(q^2) - \frac{1}{4} \right\} + \frac{c_\pi^3}{16\pi^2} \left\{ V_\pi(q^2) + 4M^2 C_0[M^2, q^2, M^2; m^2, M^2, M^2] \right\}, \quad (5)$$

where

$$V_\pi(q^2) = B_0[0; M^2, M^2] + \frac{2q^2 B_0[M^2; m^2, M^2]}{4M^2 - q^2} - \frac{(4M^2 + q^2) B_0[q^2; M^2, M^2]}{4M^2 - q^2} - \frac{m^2(4M^2 + q^2) C_0[M^2, q^2, M^2; m^2, M^2, M^2]}{4M^2 - q^2}, \quad (6)$$

with B_0 and C_0 the two- and three-point Passarino-Veltman functions [10], given in Appendix A. It can be easily verified that any dependence on the regularisation parameters Δ and Λ cancels out in Eq. (5) (as it should), thus proving the ultraviolet and infrared convergence of the renormalised loop. Using formulae from Appendix A and retaining only the

leading orders of m/M and $(m/M) \ln(m/M)$ in the B_0 functions, Eq. (5) can be rewritten in a more explicit form

$$\begin{aligned} \Gamma_\pi(q^2) \approx & -\frac{c_\pi g_\pi^2}{64\pi^2} + \frac{c_\pi}{16\pi^2(4M^2 - q^2)} \left\{ (g_\pi^2 + c_\pi^2) \left[4q^2 \left(1 - \frac{m}{M} \operatorname{arctg} \frac{M}{m} \right) - 2q^2 \frac{m^2}{M^2} \ln \frac{m}{M} \right. \right. \\ & + (4M^2 + q^2) \int_0^1 dx \ln \left(1 + \frac{q^2 x(x-1)}{M^2} \right) \left. \right] \\ & + \left[4M^2(4M^2 - q^2)c_\pi^2 - m^2(4M^2 + q^2)(g_\pi^2 + c_\pi^2) \right] C_0[M^2, q^2, M^2; m^2, M^2, M^2] \left. \right\}, \quad (7) \end{aligned}$$

with $C_0[M^2, q^2, M^2; m^2, M^2, M^2]$ given by Eq. (A8). (The q^2 -independent additive constant is unimportant here since in presenting our results we will normalise $F_{\mathcal{PT}}(Q^2 = 0) = 1$.) The vertex loops with the ρ , ω and η mesons have a structure similar to that of the pion in Eq. (5); their contributions are given in Appendix B.

Examples of the calculated PTV πNN form factor $F_{\mathcal{PT}}(Q^2)$ are shown in Fig. 2, where we display separately the contributions from the vertex loops from Fig. 1 involving π , ρ , ω and η mesons. The form factor depends on a particular relation among the generally unknown PTV meson-nucleon coupling constants c_π , c_η , c_ρ and c_ω . This is illustrated in the four panels of Fig. 2, where we used PTV constants of comparable size with various sign combinations. The results in Fig. 2 were obtained using the pseudovector (pv) structure of the strong πNN vertex, as given in Eq. (2). If instead we use the pseudoscalar (ps) πNN vertex to calculate the diagrams in Fig. 1, then only the loops containing the vector mesons ρ and ω would be different from the pv case. As a result, there is an approximate relation between the PTV πNN form factors obtained using the ps and the pv πNN vertices: the form factor obtained using the ps πNN vertex and with a certain relation among the PTV constants c_π , c_η , c_ρ and c_ω is approximately equal to that obtained using the pv vertex, but with the signs of c_ρ and c_ω changed. For example, the lower left panel in Fig. 2 shows either the form factor calculated using the pv vertex and with $c_\rho = c_\omega = -0.5c_\eta = -0.5c_\pi$ or (approximately) the form factor obtained using the ps vertex, but with $c_\rho = c_\omega = 0.5c_\eta = 0.5c_\pi$.

We can see from Fig. 2 that the contributions of the vector mesons ρ and ω to the PTV πNN form factor are larger when c_ρ and c_ω have opposite signs compared to c_π and c_η of the pseudoscalar mesons. Furthermore, for any combination of the PTV coupling constants, the ρ and ω contributions have comparable magnitudes but opposite signs. The η meson gives the smallest contribution. If the PTV coupling constants c_ρ , c_ω and c_η were all much smaller than c_π , then the resulting form factor would be approximated by the pion loop contribution alone, given by the dashed line in Fig. 2. Currently there is no strong reason to assume that c_π is dominant, or adopt any other particular relation among the PTV coupling constants (various arguments on this issue have been presented in Refs. [3, 11]). Our results in Fig. 2 indicate that a measurement of the PTV πNN form factor could be very useful for establishing such a relation. Fig. 2 also shows that for some relations among the coupling constants, the form factor may have a zero at Q^2 of the order $\sim M^2$. Although at present we cannot make a specific statement about the significance of such a zero, it might be important in some applications of the form factor. In the next two sections we will analyse in more detail the PTV πNN form factor in the low- and high-energy regions.

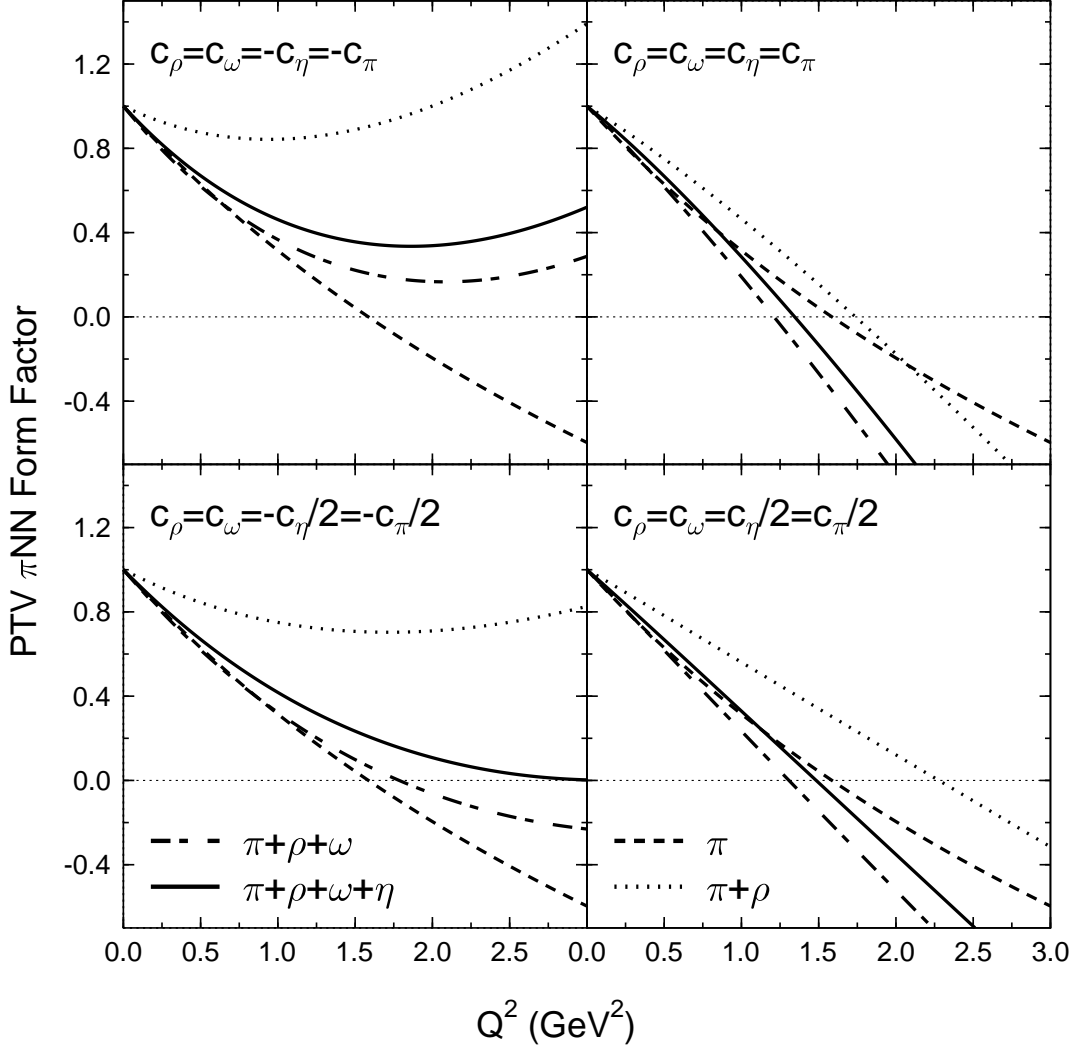


FIG. 2: Contributions of the meson loops to the P- and T-violating πNN form factor $F_{PT}(Q^2)$, defined in Eq. (4), using the indicated relations among the PTV meson-nucleon coupling constants. The total form factor is the sum of all meson contributions and is given by the solid curves.

IV. MEAN SQUARE RADIUS AND THE EFFECT ON THE NEUTRON EDM

We define the mean square radius associated with the PTV πNN interaction by analogy with the standard definition used for electromagnetic form factors:

$$\langle r_{PT}^2 \rangle = -6 \left(\frac{\partial F_{PT}}{\partial Q^2} \right)_{Q^2=0}. \quad (8)$$

The contributions to the radius from the loops involving particular mesons will be denoted by the corresponding subscripts:

$$\langle r_{PT}^2 \rangle_{\pi} \approx (0.19 - 0.00062 c_{\pi}^2) \text{ fm}^2, \quad (9)$$

$$\langle r_{\vec{p}\vec{T}}^2 \rangle_\rho \approx \left(-0.092 \pm 0.015 \frac{c_\rho}{c_\pi} + 0.00035 c_\rho^2 \right) \text{ fm}^2, \quad (10)$$

$$\langle r_{\vec{p}\vec{T}}^2 \rangle_\omega \approx \left(0.093 \mp 0.032 \frac{c_\omega}{c_\pi} - 0.00036 c_\omega^2 \right) \text{ fm}^2, \quad (11)$$

$$\langle r_{\vec{p}\vec{T}}^2 \rangle_\eta \approx \left(0.0011 - 0.026 \frac{c_\eta}{c_\pi} - 0.000018 c_\eta^2 \right) \text{ fm}^2, \quad (12)$$

where the upper (lower) sign in Eqs. (10) and (11) corresponds to the use of the pv (ps) structure of the strong πNN vertex. The leading term of the pion loop contribution can be written analytically in a compact form

$$\langle r_{\vec{p}\vec{T}}^2 \rangle_\pi = \frac{5g_\pi^2}{16\pi^2 M^2} + \mathcal{O}(c_\pi^2, m^2/M^4) = \frac{5g_A^2}{16\pi^2 F_\pi^2} + \mathcal{O}(c_\pi^2, m^2/M^4) \approx 0.22 \text{ fm}^2, \quad (13)$$

where we have used the Goldberger-Treiman relation $g_\pi F_\pi = g_A M$ (with $F_\pi = 93$ MeV being the pion decay constant and $g_A = 1.267$ the axial coupling constant), valid in leading chiral order. Neglecting the (presumably suppressed) quadratic terms in Eqs. (9-12) and adding up the leading terms, we obtain the total mean square radius associated with the PTV πNN form factor:

$$\langle r_{\vec{p}\vec{T}}^2 \rangle = \langle r_{\vec{p}\vec{T}}^2 \rangle_\pi + \langle r_{\vec{p}\vec{T}}^2 \rangle_\rho + \langle r_{\vec{p}\vec{T}}^2 \rangle_\omega + \langle r_{\vec{p}\vec{T}}^2 \rangle_\eta \approx \left(0.19 \pm 0.015 \frac{c_\rho}{c_\pi} \mp 0.032 \frac{c_\omega}{c_\pi} - 0.026 \frac{c_\eta}{c_\pi} \right) \text{ fm}^2. \quad (14)$$

This shows, in particular, that if $|c_{\rho,\omega,\eta}| \gg |c_\pi|$, then the dominant contribution to $\langle r_{\vec{p}\vec{T}}^2 \rangle$ comes almost entirely from the pion loops, in which case the explicit formula Eq. (13) can be used as a good approximation to the full result Eq. (14): $\langle r_{\vec{p}\vec{T}}^2 \rangle \approx \langle r_{\vec{p}\vec{T}}^2 \rangle_\pi$.

We can use the mean square radius to estimate the effect of the PTV πNN form factor on the neutron EDM D_n . First we will cite here some results on D_n obtained in approaches similar to ours, where we will use the recent reviews [2, 12] and references therein. The upper bound from experiments with ultra-cold neutrons is $D_n^{EXP} \leq 7.5 \times 10^{-26} e \cdot \text{cm}$, where e denotes the elementary electric charge. In the Standard Model calculations, D_n appears as a strongly suppressed perturbation effect: $D_n^{SM} \approx 10^{-32} e \cdot \text{cm}$. If a discrepancy between the Standard Model prediction and experiment is eventually established, it may indicate a P- and T-violation, or other fundamental extensions of the Standard Model. These possibilities are explored in many calculations wherein one uses EDM measurements to constrain various PTV parameters, e. g. the QCD θ -term, CP-violating quark coupling constants, etc. Examples of such model calculations, most relevant in the context of the present paper, include the following. The MIT quark bag model [13] yields the neutron dipole moment $D_n^{QM} \approx 8.2 \times 10^{-16} \theta e \cdot \text{cm}$. The estimate from the leading chiral logarithm [6] is $D_n^{\chi Log} \approx 3.6 \times 10^{-16} \theta e \cdot \text{cm}$, while the extended $SU(3)$ chiral perturbation theory calculation [15] gives to first order $D_n^{\chi PT} \approx (3.3 \pm 1.8) \times 10^{-16} \theta e \cdot \text{cm}$. In the effective lagrangian model [3] D_n is evaluated in terms of the PTV meson-nucleon coupling constants given in Eq. (3): $D_n^{EL} \approx [0.14 \bar{g}_\pi^{(0)} - 0.02 (\bar{g}_\rho^{(0)} - \bar{g}_\rho^{(1)} + \bar{g}_\rho^{(2)}) + 6 \times 10^{-3} \bar{g}_\omega^{(0)}] e \cdot \text{cm}$. Another approach [14], based on QCD sum rules, predicts $D_n^{SR} \approx 1.2 \times 10^{-16} \theta e \cdot \text{cm}$.

The aforementioned leading chiral contribution $D_n^{\chi Log}$ is obtained [6, 7, 15] from the one-pion loop correction to the PTV γNN vertex where the photon couples to the intermediate pion:

$$D_n^{\chi Log} = \frac{e c_\pi g_\pi}{4\pi^2 M} \ln \frac{M}{m}, \quad (15)$$

with effects of the PTV πNN form factor being neglected in Eq. (15). We assume that the loop integral for the neutron EDM is dominated by the region of very small four-momenta squared Q^2 of the intermediate pions. In this region the form factor $F_{\not{p}\not{T}}(Q^2) \approx 1 - \langle r_{\not{p}\not{T}}^2 \rangle Q^2/6$. If we set $Q^2 \approx m^2$ in this expansion and substitute it into the EDM pion-loop correction in place of the PTV πNN form factor, then the Q^2 dependence of the form factor does not have to be integrated. Thus we obtain an estimate for the neutron EDM

$$D_n^{FF} = D_n^{\chi \text{Log}} \left(1 + \delta_{\not{p}\not{T}}^{FF} \right), \quad (16)$$

with the correction due to the PTV πNN form factor

$$\delta_{\not{p}\not{T}}^{FF} \approx -\frac{m^2}{6} \langle r_{\not{p}\not{T}}^2 \rangle \approx -\frac{5g_\pi^2 m^2}{96\pi^2 M^2} + \mathcal{O}(c_\pi^2, m^4/M^4) \approx -2\%, \quad (17)$$

where we have used Eq. (13). We should point out that in view of the preceding simplifying assumptions, this is a rather crude estimate which may give only an approximate magnitude of the effect. A more detailed treatment must involve a careful integration of the EDM vertex loop including the PTV πNN form factor (which in turn depends on the unknown PTV meson-nucleon coupling constants, as discussed in Section III). Such a calculation falls outside the scope of this paper.

V. HIGH-ENERGY SCALE EVOLUTION OF THE PTV πNN COUPLING CONSTANT FROM THE CALLAN-SYMANZIK EQUATION

The Callan-Symanzik (or renormalisation group) equation [9, 16, 17] describes the evolution of a renormalised coupling constant $c_\pi(\mu)$, defined at a typical mass scale $\sqrt{-q^2} \sim \mu$, where, ideally, all the masses in the problem are negligible in comparison with μ :

$$\mu \frac{dc_\pi(\mu)}{d\mu} = \beta(c_\pi). \quad (18)$$

In our case it should be sufficient to take μ to be much larger than the nucleon mass M . The evolution is determined by the renormalisation-group β function $\beta(c_\pi) \equiv \beta_\pi$ which we will calculate in this section. To keep the discussion transparent, we will consider the scale evolution of the PTV πNN coupling constant in isolation, extracting the β function from the one-pion loops only and ignoring the evolution of the other coupling constants. Although these simplifications make the renormalisation group considerations somewhat formal, the results of this section should provide a useful approximation of the true behaviour of $c_\pi(\mu)$. For definiteness, throughout this section we assume that $c_\pi(\mu) > 0$. This choice of the sign does not restrict the renormalisation group considerations since, as Eq. (18) shows, $\beta(-c_\pi) = -\beta(c_\pi)$. In general, one can consider $|c_\pi(\mu)|$ without any change in the following discussion.

We will calculate the β functions for the two structures of the strong (non-PTV) πNN vertex: the pv structure, given in Eq. (2), and the ps structure. As described in Section III, the renormalised pion loops for the PTV form factor are the same using either of the two structures. However, the β functions are different in these two cases, as will be shown below. We use dimensional regularisation to calculate the loop integrals at a space-time dimension D and apply the modified minimal subtraction procedure. In this scheme, the β function at one-loop level can be extracted as the coefficient at the term $1/(4-D) - \gamma_E/2 + \ln(4\pi)/2 \equiv \Delta/2$

which enters into the bare coupling constant in order to cancel the UV divergences of the loop integrals [9, 17, 18]. The Δ term appears in our calculation only through the functions B_0 in the *unrenormalised* loop integrals, see Eq. (A3). Thus we obtain:

$$\beta_\pi^{(pv)} = \frac{3g_\pi^2}{16\pi^2}c_\pi - \frac{1}{8\pi^2}c_\pi^3, \quad (19)$$

using the pv strong πNN vertices in the loops, and

$$\beta_\pi^{(ps)} = -\frac{g_\pi^2}{8\pi^2}c_\pi - \frac{1}{8\pi^2}c_\pi^3, \quad (20)$$

using the ps vertices.

Integrating the Callan-Symanzik equation (18) between mass scales μ_1 and μ_2 , with the β functions Eq. (19) and Eq. (20), we obtain the solution

$$\left(\frac{\mu_2}{\mu_1}\right)^A = \frac{c_\pi(\mu_2)}{c_\pi(\mu_1)} \sqrt{\frac{1 + \frac{B}{A}c_\pi^2(\mu_1)}{1 + \frac{B}{A}c_\pi^2(\mu_2)}}, \quad (21)$$

where

$$A = A^{(pv)} = \frac{3g_\pi^2}{16\pi^2} \approx 3.25, \quad B = -\frac{1}{8\pi^2} \approx -0.013, \quad (22)$$

and

$$A = A^{(ps)} = -\frac{g_\pi^2}{8\pi^2} \approx -2.16, \quad B = -\frac{1}{8\pi^2} \approx -0.013, \quad (23)$$

using the pv and ps strong πNN vertices, respectively.

If we work at moderate mass scales μ , where $|Bc_\pi^2(\mu)/A| \ll 1$, we can retain only the leading order in the β function,

$$\beta_\pi \approx A c_\pi, \quad (24)$$

for which an approximate solution of Eq. (18) can be written

$$c_\pi(\mu) \approx c_\pi(\mu_0) \left(\frac{\mu}{\mu_0}\right)^A, \quad (25)$$

where μ_0 is some ‘‘initial’’ renormalisation point (one may choose it to be of the order of the nucleon mass, $\mu_0 \sim M$, assuming that $c_\pi(\mu_0 \sim M)$ has a magnitude relevant to EDM measurements or to other PTV experiments).

Consider first the calculation using the pv strong πNN vertex in the loops. In this case $A = A^{(pv)} > 0$, see Eq. (22), hence the approximate solution Eq. (25) describes a growth of $c_\pi(\mu)$ with μ . For a sufficiently large scale μ the value of $c_\pi(\mu)$ could become so big that the β function Eq. (19) could vanish. Then the approximate solution Eq. (25) would no longer be valid. Instead, Eq. (18) shows that $c_\pi(\mu \rightarrow \infty)$ would tend to a fixed point c_π^* determined from the condition $\beta_\pi^{(pv)}(c_\pi^*) = 0$. In the vicinity of the fixed point

$$\beta_\pi^{(pv)} \approx a(c_\pi^* - c_\pi), \quad c_\pi^* = \sqrt{\frac{3}{2}}g_\pi \approx 16, \quad a = \frac{3g_\pi^2}{8\pi^2} \approx 6.5, \quad (26)$$

and the solution of Eq. (18) describes how $c_\pi(\mu)$ approaches c_π^* :

$$c_\pi^* - c_\pi(\mu) \sim \left(\frac{\mu}{\mu_0}\right)^{-a}. \quad (27)$$

Recalling that c_π is proportional to the CP-violating θ term which could be included in a QCD lagrangian [2, 6], the evolution of $c_\pi(\mu)$ in Eq. (25) is compatible with an extremely small $\theta \leq 3 \times 10^{-10}$ [1, 2], as extracted from EDM measurements at low energies. In this scenario, obtained in our model using the pv strong πNN vertex, an initially small value of c_π grows as a positive power of the mass scale μ and may eventually reach a fixed value c_π^* . Using Eq. (25) with $A = A^{(pv)} \approx 3.25$, $\mu_0 \approx M$, $c_\pi(M) \leq 7 \times 10^{-12}$ [1] and $c_\pi(\mu) = g_\pi/\sqrt{2}$ (the point at which $\beta_\pi^{(pv)}$ of Eq. (19) reaches its maximum and starts decreasing), one can estimate that the fixed point c_π^* would be approached at energies above $\mu \sim 5$ TeV.

Now consider the calculation with the ps strong πNN vertices in the loops for the PTV form factor. A qualitatively different behaviour of $c_\pi(\mu)$ obtains in this case. The β function Eq. (20) remains negative for all c_π , and the general solution of the renormalisation group equation Eq. (18) is well approximated by Eq. (25). Since $A = A^{(ps)} < 0$, see Eq. (23), the solution Eq. (25) describes a gradual decrease and eventual vanishing of $c_\pi(\mu)$ as $\mu \rightarrow \infty$.

Whether one of these two contrasting scenarios of the high-energy scale evolution of $c_\pi(\mu)$ is correct should be, in principle, clarified by experiment. An important caveat here is that the dynamics at high energies will certainly involve hadron resonances, quark-gluon and other – possibly supersymmetric – degrees of freedom not included in our model (for a recent review, see [2] and references therein). These degrees of freedom would probably influence the high-energy evolution of $c_\pi(\mu)$, which in turn could change the discussion presented in this section.

VI. SUMMARY

We have described a calculation of the form factor associated with the parity and time-reversal violating (PTV) pion-nucleon coupling. The form factor is generated in our model by one-loop vertex corrections involving nucleon, pion, ρ -, ω - and η -meson degrees of freedom. The interaction of these hadrons is described by a phenomenological lagrangian consisting of a strong interaction part and a PTV part. The latter is determined by several PTV meson-nucleon coupling constants, all of which are in general unknown, as are their relative orders of magnitude.

One result of the present calculation is that by measuring the PTV πNN form factor, it should in principle be possible to constrain this set of the PTV meson-nucleon coupling constants, since different relations among them lead to distinct Q^2 dependences of the form factor, as shown in Fig. 2. The experimental feasibility of such a measurement is certainly a challenging problem in its own right, and we have left an investigation of this question outside the scope of the present paper. We found that the PTV πNN form factor generated by the loops with the strong pv πNN vertex is related in a simple way to that generated by the loops with the strong ps vertex: these two form factors are converted into each other by reversing the signs of the PTV couplings of the vector mesons.

We have analysed the low-energy characteristics of the PTV pion-nucleon interaction by evaluating the mean square radius associated with its form factor. It turned out that, if all the PTV coupling constants are of the same order of magnitude (or at least if the pion-nucleon constant is not much smaller than the others), then the contributions of the ρ and ω mesons almost completely cancel each other, and that of the η meson is suppressed. As a result, the mean square radius can be well approximated by the pion-loop contribution alone, which can be given by a simple expression Eq. (13). This is consistent with the intuitive expectation that the pion cloud should dominate the low-energy features of the interaction.

The simplified estimate in Section IV suggests that the effect of the PTV πNN form factor on the neutron EDM is very small. A more definite statement can be made on the basis of a detailed calculation of the loop integrals for the EDM, including the full Q^2 -dependence of the PTV πNN form factor, which was not pursued in the present paper.

It has been shown elsewhere [6, 15] that the PTV pion-nucleon coupling constant is proportional to the CP-violating θ term which can be added to the QCD lagrangian. The current estimates of θ based on measurements of EDMs of the neutron and various atoms and molecules, yield an extremely small upper limit $|\theta| < 3 \times 10^{-10}$, which presents a long-standing puzzle [2]. Since the value of θ may be energy-scale dependent (for example, yielding appreciable CP-violating effects at sufficiently high energies), we have considered in our model possible scenarios of the evolution of the PTV πNN coupling constant $c_\pi(\mu)$ with the energy scale μ . To this end, we employed renormalisation group techniques, with several simplifying assumptions. Being used in the framework of a model, results of such an analysis are to some extent speculative. Nevertheless, we found in Section V an intriguing possibility that, in the calculation with the pv strong πNN vertex, the PTV πNN coupling constant relevant to very high energy scales may be significantly larger than the tiny value extracted from the low-energy EDM measurements. In the ultraviolet limit $\mu \rightarrow \infty$, $c_\pi(\mu)$ may eventually reach a fixed value c_π^* , Eq. (26), of a “natural” size.

APPENDIX A: PASSARINO-VELTMAN FUNCTIONS

In this appendix we give the scalar Passarino-Veltman functions [10, 19] B_0 and C_0 entering into the expressions for the loop integrals. The functions are defined as D-dimensional integrals

$$B_0[p^2; m_1^2, m_2^2] \equiv \frac{(2\pi\Lambda)^{4-D}}{i\pi^2} \int d^D q \left\{ [q^2 - m_1^2 + i0][(q+p)^2 - m_2^2 + i0] \right\}^{-1}, \quad (\text{A1})$$

$$C_0[p_1^2, p_2^2, (p_1 + p_2)^2; m_1^2, m_2^2, m_3^2] \equiv \frac{(2\pi\Lambda)^{4-D}}{i\pi^2} \int d^D q \left\{ [q^2 - m_1^2 + i0][(q+p_1)^2 - m_2^2 + i0][(q+p_1+p_2)^2 - m_3^2 + i0] \right\}^{-1}, \quad (\text{A2})$$

where Λ is an arbitrary cutoff mass introduced to keep the dimensions of B_0 and C_0 independent of D (upon renormalisation, the loop integrals do not depend on Λ , and the limit $D \rightarrow 4$ can also be taken without encountering divergences). Eqs. (A1) and (A2) can be reduced to one- and two-dimensional integrals which are either evaluated numerically or expressed via logarithm and dilogarithm functions. We have

$$B_0[p^2; m_1^2, m_2^2] = \Delta + B_0^f[p^2; m_1^2, m_2^2], \quad (\text{A3})$$

where

$$\Delta \equiv \frac{2}{4-D} - \gamma_E + \ln(4\pi), \quad \gamma_E \approx 0.5772 \text{ (Euler's constant)}. \quad (\text{A4})$$

is a divergent (in the limit $D \rightarrow 4$) constant typical for the modified minimal subtraction procedure, and

$$B_0^f[p^2; m_1^2, m_2^2] = - \int_0^1 dx \ln \left(\frac{x^2 p^2 - x(p^2 - m_2^2 + m_1^2) + m_1^2 - i0}{\Lambda^2} \right) + \mathcal{O}(D-4), \quad (\text{A5})$$

is a finite (ultraviolet convergent) one-dimensional integral.

In our loop integrals we encounter only C_0 functions with $p_1^2 = (p_1 + p_2)^2 = M^2$ and $p_2^2 = q^2$, which can be reduced to convergent two-dimensional integrals

$$C_0[M^2, q^2, M^2; m_1^2, m_2^2, m_3^2] = -\int_0^1 dx \int_0^{1-x} dy \left\{ M^2(x+y)^2 - xyq^2 - M^2(x+y) - x(m_1^2 - m_2^2) - y(m_1^2 - m_3^2) + m_1^2 - i0 \right\}^{-1}. \quad (\text{A6})$$

The B_0 and C_0 functions from the pion loops Eq. (5) can be further simplified:

$$B_0^f[q^2; M^2, M^2] = -2 \ln \frac{M}{\Lambda} - \int_0^1 dx \ln \left(1 + \frac{q^2 x(x-1)}{M^2} - i0 \right), \quad (\text{A7})$$

$$C_0[M^2, q^2, M^2; m^2, M^2, M^2] = \frac{x_q}{M^2(1-x_q^2)} \left\{ \ln(x_q) \left[2 \ln(1+x_q) - \frac{1}{2} \ln x_q - 2 \ln \frac{m}{M} \right] + \frac{\pi^2}{6} + 2 \text{Li}_2(-x_q) \right\}, \quad (\text{A8})$$

where $x_q = \left[\sqrt{(q^2 - 4M^2)/(q^2 + i0)} - 1 \right] \cdot \left[\sqrt{(q^2 - 4M^2)/(q^2 + i0)} + 1 \right]^{-1}$ and the dilogarithm (Spence) function is

$$\text{Li}_2(x) = -\int_0^1 dy \frac{\ln(1-xy)}{y} \quad (|\arg(1-x)| < \pi). \quad (\text{A9})$$

The following special cases are useful in deriving Eqs. (7) and (13):

$$B_0^f[q^2; M^2, M^2] = -2 \ln \frac{M}{\Lambda} + \frac{q^2}{6M^2} + \mathcal{O}\left(\frac{q^4}{M^4}\right) \quad (|q^2| \ll M^2), \quad (\text{A10})$$

$$B_0^f[M^2; m^2, M^2] = -2 \ln \frac{M}{\Lambda} + 2 \left(1 - \frac{m}{M} \arctg \frac{M}{m} \right) - \frac{m^2}{M^2} \ln \frac{m}{M} + \mathcal{O}\left(\frac{m^2}{M^2}\right), \quad (\text{A11})$$

$$C_0[M^2, 0, M^2; m^2, M^2, M^2] = \frac{1}{M^2} \ln \frac{m}{M} + \mathcal{O}\left(\frac{m^2}{M^4}\right). \quad (\text{A12})$$

APPENDIX B: LOOP INTEGRALS WITH THE ρ , ω AND η MESONS

In this appendix we give explicit formulae for the renormalised loop diagrams with ρ , ω and η mesons, where for brevity we will retain only the dominant linear terms $\sim c_{\pi, \rho, \omega, \eta}$, marking them with a superscript “(1)”. The contribution from the η meson equals

$$\Gamma_\eta^{(1)}(q^2) = \frac{c_\eta g_\pi g_\eta q^2}{8\pi^2(4M^2 - q^2)} \left\{ V_\eta(q^2) - B_0[M^2; M^2, m_\eta^2] \right\} + \frac{c_\pi g_\eta^2}{16\pi^2} \left\{ V_\eta(q^2) - B_0[0; M^2, M^2] + \frac{1}{4} \right\}, \quad (\text{B1})$$

where

$$V_\eta(q^2) = B_0[q^2; M^2, M^2] + m_\eta^2 C_0[M^2, q^2, M^2; m_\eta^2, M^2, M^2]. \quad (\text{B2})$$

The contributions from the ω and ρ mesons read

$$\begin{aligned}
\Gamma_\omega^{(1)}(q^2) = & -\frac{c_\pi g_\omega^2}{384M^4\pi^2} \left(48M^4 + 120\kappa_\omega M^4 + 54\kappa_\omega^2 M^4 + 12\kappa_\omega^2 M^2 m_\omega^2 + 8M^2 q^2 \right. \\
& + 24\kappa_\omega M^2 q^2 + 10\kappa_\omega^2 M^2 q^2 + \kappa_\omega^2 m_\omega^2 q^2 \left. \right) \\
& - \frac{g_\omega}{128M^4\pi^2} \left\{ c_\pi g_\omega \left(16M^4 + 48\kappa_\omega M^4 + 20\kappa_\omega^2 M^4 + 2\kappa_\omega^2 M^2 m_\omega^2 + 4M^2 q^2 \right. \right. \\
& - 3\kappa_\omega^2 M^2 q^2 + \kappa_\omega^2 m_\omega^2 q^2 \left. \left. \right) + c_\omega g_\pi q^2 \left(4M^2 + 6\kappa_\omega M^2 - \kappa_\omega m_\omega^2 \right) \right\} B_0[0; M^2, M^2] \\
& - \frac{g_\omega q^2}{128M^4\pi^2(4M^2 - q^2)} \left\{ c_\pi g_\omega \left(4M^2 + \kappa_\omega^2 m_\omega^2 \right) + c_\omega g_\pi \left(4M^2 - \kappa_\omega m_\omega^2 \right) \right\} B_0[M^2; M^2, m_\omega^2] \\
& + \frac{g_\omega}{128M^2\pi^2(4M^2 - q^2)} \left\{ c_\pi g_\omega \left(64M^4 + 192\kappa_\omega M^4 + 80\kappa_\omega^2 M^4 \right. \right. \\
& + 8\kappa_\omega^2 M^2 m_\omega^2 - 48\kappa_\omega M^2 q^2 - 32\kappa_\omega^2 M^2 q^2 + 2\kappa_\omega^2 m_\omega^2 q^2 + 3\kappa_\omega^2 q^4 \left. \left. \right) \right. \\
& + 2c_\omega g_\pi q^2 \left(8M^2 + 12\kappa_\omega M^2 - 2\kappa_\omega m_\omega^2 - 3\kappa_\omega q^2 \right) \left. \right\} B_0[q^2; M^2, M^2] \\
& + \frac{g_\omega}{64M^2\pi^2(4M^2 - q^2)} \left\{ c_\pi g_\omega \left(64M^6 + 32M^4 m_\omega^2 + 96\kappa_\omega M^4 m_\omega^2 \right. \right. \\
& + 32\kappa_\omega^2 M^4 m_\omega^2 + 4\kappa_\omega^2 M^2 m_\omega^4 - 48M^4 q^2 - 24\kappa_\omega M^2 m_\omega^2 q^2 - 16\kappa_\omega^2 M^2 m_\omega^2 q^2 \\
& + \kappa_\omega^2 m_\omega^4 q^2 + 8M^2 q^4 + 2\kappa_\omega^2 m_\omega^2 q^4 \left. \left. \right) \right. \\
& + 2c_\omega g_\pi m_\omega^2 q^2 \left(4M^2 + 8\kappa_\omega M^2 - \kappa_\omega m_\omega^2 - 2\kappa_\omega q^2 \right) \left. \right\} C_0[M^2, q^2, M^2; m_\omega^2, M^2, M^2], \quad (\text{B3})
\end{aligned}$$

$$\begin{aligned}
\Gamma_\rho^{(1)}(q^2) = & - \left(\Gamma_\omega^{(1)}(q^2) \right)_{m_\omega \rightarrow m_\rho, c_\omega \rightarrow c_\rho, g_\omega \rightarrow g_\rho, \kappa_\omega \rightarrow \kappa_\rho} \\
& + \frac{g_{\rho\pi} c_\rho g_\pi (m^2 - M^2)}{32M^2\pi^2} \left\{ 1 + B_0[0; m^2, M^2] \right\} - \frac{g_{\rho\pi} c_\pi g_\rho (\kappa_\rho m^2 - 4M^2 - \kappa_\rho m_\rho^2)}{16M^2\pi^2} B_0[0; m^2, m_\rho^2] \\
& + \frac{g_{\rho\pi} c_\rho g_\pi}{32\pi^2} \left\{ \frac{m^2}{M^2} B_0[0; m^2, m^2] - B_0[0; M^2, M^2] \right\} + \frac{g_{\rho\pi} c_\rho g_\pi (M^2 - m_\rho^2)}{16M^2\pi^2} B_0[0; M^2, m_\rho^2] \\
& - \frac{g_{\rho\pi}}{32M^2\pi^2(4M^2 - q^2)} \left\{ c_\pi g_\rho q^2 \left(\kappa_\rho m^2 - 8M^2 - 4\kappa_\rho M^2 - \kappa_\rho m_\rho^2 \right) \right. \\
& + 2c_\rho g_\pi \left(2m^2 M^2 + 2M^2 m_\rho^2 - m^2 q^2 - 2M^2 q^2 \right) \left. \right\} B_0[M^2; m^2, M^2] \\
& + \frac{g_{\rho\pi}}{32M^2\pi^2(4M^2 - q^2)} \left\{ c_\pi g_\rho q^2 \left(8M^2 + 4\kappa_\rho M^2 + \kappa_\rho m_\rho^2 - \kappa_\rho m^2 \right) \right. \\
& + 2c_\rho g_\pi \left(2m^2 M^2 + 2M^2 m_\rho^2 + 2M^2 q^2 - m_\rho^2 q^2 \right) \left. \right\} B_0[M^2; M^2, m_\rho^2] \\
& - \frac{g_{\rho\pi}}{4\pi^2(4M^2 - q^2)} \left\{ c_\pi g_\rho \left(4M^2 + \kappa_\rho m_\rho^2 + q^2 + \kappa_\rho q^2 - \kappa_\rho m^2 \right) \right. \\
& + c_\rho g_\pi \left(m^2 - m_\rho^2 + q^2 \right) \left. \right\} B_0[q^2; m^2, m_\rho^2] \\
& + \frac{g_{\rho\pi}}{8\pi^2(4M^2 - q^2)} \left\{ c_\pi g_\rho \left(8M^2 m_\rho^2 - 8m^2 M^2 + \kappa_\rho m_\rho^4 - \kappa_\rho m^4 + 4m^2 q^2 \right. \right. \\
& + 2\kappa_\rho m^2 q^2 - 8M^2 q^2 - \kappa_\rho q^4 \left. \left. \right) \right. \\
& + c_\rho g_\pi \left(m^2 + m_\rho^2 - q^2 \right) \left(m^2 - m_\rho^2 + q^2 \right) \left. \right\} C_0[M^2, q^2, M^2; M^2, m^2, m_\rho^2], \quad (\text{B4})
\end{aligned}$$

with B_0 and C_0 defined in Appendix A. To facilitate the calculation of the loop integrals, we used the computer package “FeynCalc” [20].

-
- [1] I. B. Khriplovich and S. K. Lamoreaux, *CP Violation Without Strangeness* (Springer-Verlag, 1997).
 - [2] M. Pospelov and A. Ritz, *Ann. of Phys.* **318**, 119 (2005).
 - [3] C.-P. Liu and R. G. E. Timmermans, *Phys. Rev. C* **70**, 055501 (2004).
 - [4] J. D. Bjorken and S. D. Drell, *Relativistic Quantum Fields* (McGraw-Hill, 1965).
 - [5] Particle Data Group: W.-M. Yao et al., *J. Phys. G* **33**, 1 (2006).
 - [6] R. J. Crewther, P. Di Vecchia, G. Veneziano, and E. Witten, *Phys. Lett. B* **88**, 123 (1979) [Erratum: *Phys. Lett. B* **91**, 487 (1980)].
 - [7] W.H. Hockings and U. van Kolck, *Phys. Lett. B* **605**, 273 (2005).
 - [8] G. ‘t Hooft and M. Veltman, *Nucl. Phys. B* **44**, 189 (1972); B. de Wit and J. Smith, *Field Theory in Particle Physics*, v. 1, ch. 8, 9 (Elsevier Science Publishers, 1986).
 - [9] S. Weinberg, *The Quantum Theory of Fields*, v. 2, ch. 18 (Cambridge University Press, 1995).
 - [10] G. ‘t Hooft and M. Veltman, *Nucl. Phys. B* **153**, 365 (1979); G. Passarino and M. Veltman, *Nucl. Phys. B* **160**, 151 (1979).
 - [11] V. P. Gudkov, X.-G. He, and B. H. J. McKellar, *Phys. Rev. C* **47**, 2365 (1993); M. Pospelov, *Phys. Lett. B* **530**, 123 (2002).
 - [12] R. G. E. Timmermans, Electric dipole moments and the search for T-violation, talk at the 9-th Conference on Intersections of Particle and Nuclear Physics, CIPANP 2006, Rio Grande, May 30 - June 3, 2006; to be published by AIP.
 - [13] V. Baluni, *Phys. Rev. D* **19**, 2227 (1979).
 - [14] M. Pospelov and A. Ritz, *Nucl. Phys. B* **573**, 177 (2000).
 - [15] A. Pich and E. de Rafael, *Nucl. Phys. B* **367**, 313 (1991).
 - [16] C. G. Callan, *Phys. Rev. D* **2**, 1541 (1970); K. Symanzik, *Comm. Math. Phys.* **18**, 227 (1970); K. Wilson, *Phys. Rev. D* **3**, 1818 (1971).
 - [17] M. E. Peskin and D. V. Schroeder, *An Introduction to Quantum Field Theory*, ch. 12 (Westview Press, 1995).
 - [18] G. ‘t Hooft, *Nucl. Phys. B* **61**, 455 (1973).
 - [19] H. Anlauf, *Radiative Corrections in Gauge Theories* (lectures given at the Adriatic School on Particle Physics, Split, Sept. 11-21 2001), unpublished.
 - [20] R. Mertig, M. Böhm, A. Denner, *Comp. Phys. Comm.* **64**, 345 (1991).